Theory of Rare-Earth Electronic Structure and Spectroscopy

Michael F. Reid[a,b,c]

[a] *Department of Physics and Astronomy, University of Canterbury, PB4800, Christchurch 8140, New Zealand*
[b] *The Dodd-Walls Centre for Quantum and Photonic Technologies*
[c] *The MacDiarmid Institute for Advanced Materials and Nanotechnology*

Abstract

Current theoretical understanding of electronic structure and spectroscopy of rare-earth ions in a condensed-matter environment is reviewed. The development of the crystal-field effective Hamiltonian for the $4f^n$ configuration, and its extension to the $4f^{n-1}5d$ configuration, is discussed. The addition of hyperfine and magnetic interactions is reviewed, and the use of magnetic-splitting data to improve crystal-field fitting is discussed. The development of the modeling of transition intensities, both for transitions between crystal-field levels, and transitions between J multiplets, is reviewed. The superposition model is presented as an analysis technique for both crystal-field and transition-intensity parametrizations. Developments in ab-initio calculations, and their possible impact on the field, are discussed.

Published In: Bunzli JCG; Pecharsky VK (Ed.), Handbook on the Physics and Chemistry of Rare Earths, Vol 50, 47-64, 2016. Amsterdam: North Holland.
`http://dx.doi.org/10.1016/bs.hpcre.2016.09.001`

Keywords: spectroscopy, electronic structure, crystal-field, transition intensity, magnetic fields, ab initio

Email address: `mike.reid@canterbury.ac.nz` (Michael F. Reid)

Contents

List of Figures

List of Tables

List of symbols

A^{λ}_{tp}	crystal-field level intensity parameter
α, β, γ	parameter for two-body Coulomb interactions
B^k_q	crystal-field parameter
$\bar{B}_k(R_0)$	intrinsic crystal-field parameter for a ligand at R_0
$C^{(k)}_q$	many-electron spherical tensor operator
$D^{(k)}_q$	dipole operator
$D_{\mathrm{eff},q}$	effective dipole operator
$\Delta_E(\mathrm{fd})$	energy difference between configurations
E_{avg}	average energy of configuration barycenter above the ground state.
F^k	Slater parameter for direct Coulomb interaction
G^k	Slater parameter for exchange Coulomb interaction
g	magnetic splitting parameter or tensor
H	full Hamiltonian
H_{cf}	crystal-field Hamiltonian
H_{d}	d-electron portion of the Hamiltonian
H_{eff}	effective Hamiltonian
$L^{(1)}_q$	orbital angular momentum operator
M	model space for effective Hamiltonian
$M^{(1)}_q$	magnetic-dipole operator
M^h	spin-spin and spin-other-orbit parameter
Ω_{λ}	J-multiplet intensity parameter
P^k	electrostatically-correlated spin-orbit interaction
$S^{(1)}_q$	spin angular momentum operator
T^i	parameter for three-body Coulomb interaction
U^{λ}_{p+q}	unit tensor operator
ζ	spin-orbit interaction parameter

1. Introduction

This Chapter gives a perspective on current understanding of electronic energy levels and transition intensities of rare-earth ions, in a condensed matter environment, either solid state or solution. The intention is not to give a detailed history, but to put current understanding into a somewhat historical perspective. This perspective is shaped by my participation in the field from the late 1970s. My description of earlier times is based on what I found important to my understanding and on personal interactions with many of the key people mentioned in this Chapter.

The theoretical techniques that matured during the 1960s, and were refined in subsequent decades, were important in the development of laser, phosphor, and scintillator materials that are currently ubiquitous, and one might speculate that modern developments will be important for new applications such as quantum information and bio-imaging.

There are many reviews of different aspects of the theory of rare-earth spectroscopy, including a number of articles in this Handbook [1, 2, 3], and it is not the intention of this article to cover all of the details.

Early work on crystal-field theory, beginning with Bethe's 1929 article [4], assumed that the effect of the crystal was due to electrostatic interactions. Though this assumption was later shown to be highly inaccurate, this work was notable in establishing the importance of the application of point group theory in spectroscopy, allowing the analysis of complex spectra. The 1940s and 1950s saw steady development of theory, with applications not only to optical and magnetic susceptibility data, but also magnetic resonance [5].

A key factor that drove the development of the "standard model" of crystal-field theory for the $4f^n$ configuration was high-quality optical spectral data, from laboratories such as Dieke's [6]. This data provided enough spectroscopic information to make accurate calculations both possible and worthwhile. At the same time, developments in computer technology made calculations requiring the diagonalization of large matrices tractable.

The theoretical developments led to two key advances:

1. A Hamiltonian that allowed accurate explanations of energy levels.
2. A transition-intensity model that was also crucial to optical applications development.

This Chapter will review those models, and discuss some recent advances in parametrization techniques and ab-initio calculations.

2. Energy Levels

The "crystal-field" model is often misunderstood. It's early origins in calculations that treated crystals as an array of point charges has obscured the generality of the method. We have come to understand the crystal-field model as a particular case of an "effective Hamiltonian". Effective Hamiltonians and effective operators are defined within a *model space* M. For our purposes the

model space will often be the $4f^n$ configuration, sometimes supplemented by the $4f^{n-1}5d$ configuration.

Suppose that the eigenvalue equation for the full Hamiltonian H is given by:

$$H|a\rangle = E_a|a\rangle. \tag{1}$$

The aim is to define an *effective Hamiltonian* $H_{\rm eff}$ that gives identical *eigenvalues* E_a for model-space eigenstates $|a_0\rangle$, i.e.

$$H_{\rm eff}|a_0\rangle = E_a|a_0\rangle. \tag{2}$$

The spin Hamiltonians used in EPR analyses [5] are examples of effective Hamiltonians. In the simplest spin-Hamiltonian case, any doublet can be treated as if it has a spin of 1/2. Clearly, in that case the "effective spin" quantum numbers are not the physical quantum numbers of the electrons, though they can be related (see Sections 2.3, 2.4).

An effective Hamiltonian may be related to the full Hamiltonian by a linear-algebra transformation between the full space and model space. Effective operators (such as an effective dipole moment operator — see Section 3.2) may also be defined. For further details see Appendix A of Ref. [7].

2.1. Free Ion and "Crystal-Field" interactions

The effective Hamiltonian acting within the $4f^n$ configuration is commonly written [8]:

$$\begin{aligned} H_{\rm eff} &= E_{\rm avg} + \sum_{k=2,4,6} F^k f_k + \zeta_f A_{\rm so} + \alpha L(L+1) + \beta G(G_2) + \gamma G(R_7) \\ &+ \sum_{i=2,3,4,6,7,8} T^i t_i + \sum_{h=0,2,4} M^h m_h + \sum_{k=2,4,6} P^k p_k + \sum_{k=2,4,6} B^k_q C^{(k)}_q . \end{aligned} \tag{3}$$

$E_{\rm avg}$ is the energy difference between the ground-state energy and the configuration center of gravity (barycenter) and is included to allow the ground-state energy to be set to zero. The Coulomb interaction between the 4f electrons is parametrized by the radial electrostatic integrals, F^k, which multiply the angular part of the electrostatic interaction, f_k. The coupling of the electron spin magnetic moment and the magnetic field originating in the orbital motion of the electron is represented by the spin-orbit coupling constant, ζ_f, which multiplies the angular part of the spin-orbit interaction, $A_{\rm so}$.

Higher-order terms in the Hamiltonian include two-electron Coulomb correlation contributions represented by parameters α, β, and γ and three-electron Coulomb correlation contributions are parametrized by the T_i. The M^h and P^k parametrize higher-order spin-dependent effects. Though their effects are subtle, the introduction of these parameters was essential. Without the two- and three-body correlation effects and higher-order magnetic effects, errors in the treatment of the free-ion part of the Hamiltonian make it impossible to fit the crystal field accurately. In complex systems the J multiplets can even be in the

wrong order [9]. Judd's analysis of the three-body operators [10] showed that some of the parameters could be eliminated, since they would only have contributions at third order in perturbation theory. This reduction in the number of parameters was crucial in making parameter fits tractable.

The terms in the Hamiltonian that represent the non-spherical part of the interaction with the crystal are modeled using the so-called crystal-field Hamiltonian. It is important to recognize that this Hamiltonian is not restricted to electrostatic effects, which are only a fraction of the total crystal-field effect [11]. When the parameters are fitted to experimental energies, their values reflect all one-electron non-spherical interactions. The crystal-field Hamiltonian is expressed in Wybourne [12] notation as

$$H_{\mathrm{cf}} = \sum_{k,q} B_q^k C_q^{(k)}, \tag{4}$$

where the B_q^k parameters define the one-electron crystal-field interaction and the $C_q^{(k)}$ are spherical tensor operators for the $4f^n$ configuration. For f^n configurations, $k = 2, 4, 6$, and non-zero values of q depend upon the site symmetry of the rare-earth ion in the host lattice. The total number of crystal field parameters ranges from 27 parameters for C_1 or C_i symmetry, down to only two parameters for octahedral or cubic symmetry.

Most calculations use basis vectors of the form $|\alpha SLJM\rangle$, where the last four labels are the total spin angular momentum, total orbital angular momentum, total angular momentum, and the projection of the total angular momentum along the quantization axis. The label α distinguishes basis states with the same SL quantum numbers. These extra labels are defined by the group theory developed by Racah, and the calculation of matrix elements make use of these powerful techniques. See, for example, Refs. [13, 12].

The Hamiltonian parameters may be fitted to the energies of the sharp transitions within the $4f^n$ configuration, e.g. see Ref. [8, 1, 7]. The largest splittings are caused by the Coulomb interaction, which splits the configuration into SL terms separated by the order of 10^4 cm^{-1}. The spin-orbit interaction splits these terms into SLJ multiplets separated by the order of 10^3 cm^{-1} and mixes states with different S and L quantum numbers. Finally, the crystal-field interaction splits the multiplets in to mixtures of the $|\alpha SLJM\rangle$ basis states, split by order of 10^2 cm^{-1}.

The crystal-field parameters vary between crystals, since they depend on the site symmetry and the nature of other ions in the crystal. However, the free-ion interactions, and therefore the positions of the multiplets, are almost independent of the crystal. Since the crystal field generally splits the J multiplets by less than their separation, it is useful to construct, a "Dieke" or "Dieke-Carnall" diagram for the entire series of trivalent ions to give an overview of the energy-levels of the $4f^n$ configuration (Fig. 1). Studies such the exhaustive analysis of rare-earth ions in LaF_3 by Carnall and co-workers [8] shows that both free-ion and crystal-field parameters have systematic trends across the series.

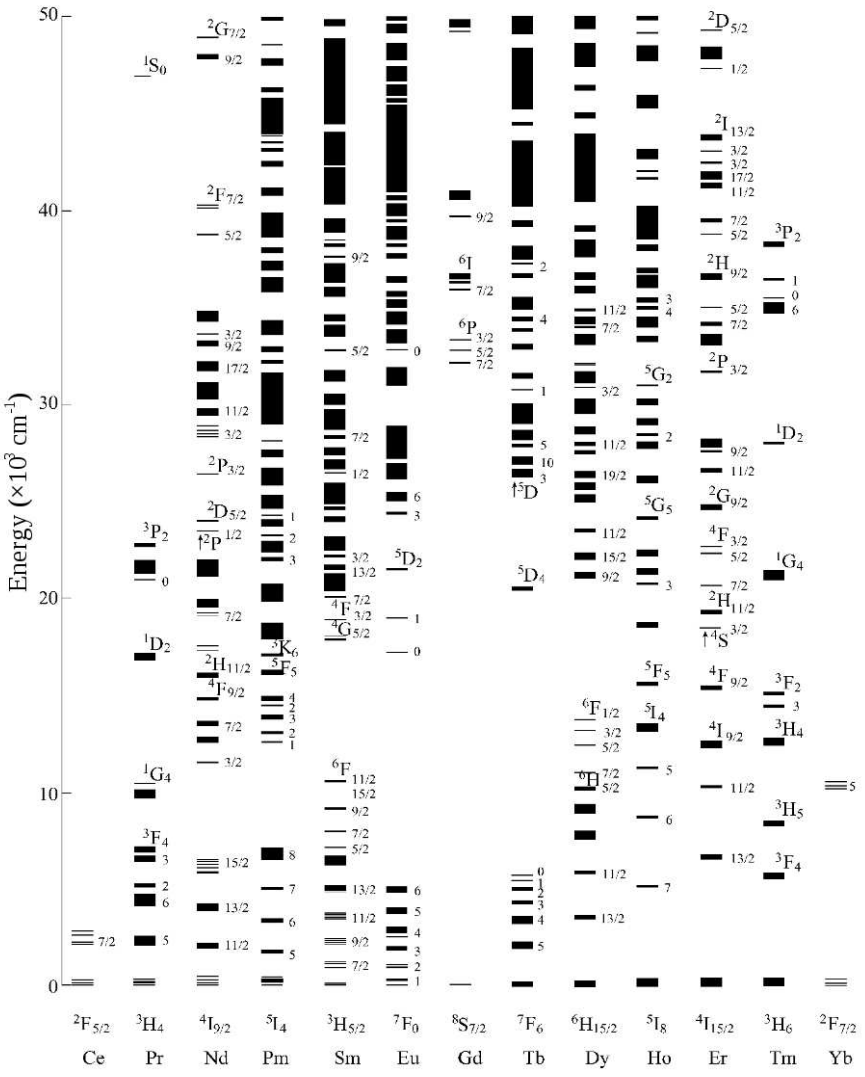

Figure 1: Dieke diagram for trivalent rare-earth ions in LaF_3, after [8, 7]. The configurations range from $4f^1$ (Ce^{3+}) to $4f^{13}$ (Yb^{3+}). The lines indicate the energies of the multiplets, with the widths of the lines representing the crystal-field splittings of the multiplets.

2.2. The $4f^{n-1}5d$ configuration

The crystal-field model for the $4f^{n-1}$ configuration may be extended in a straight-forward way to the higher-energy $4f^{n-1}5d$ configuration. Early calculations [14] for this configuration date back to the 1960's, on divalent ions, where the $4f^{n-1}5d$ configuration has lower energy than in trivalent ions. However, it was the availability of vacuum ultraviolet synchrotron sources, and the investigation of wide band-gap materials such as fluorides, that generated enough data to make detailed analysis across the series possible [15, 16].

For the $4f^{n-1}5d$ configuration we must add 5d spin-orbit and crystal-field parameters, the direct (F) and exchange (G) Coulomb interaction between the f and d electrons, and a parameter $\Delta_E(\mathrm{fd})$ representing the average energy difference between the configurations. The additional terms are [3]:

$$\begin{aligned} H_{\mathrm{d}} &= \Delta_E(\mathrm{fd}) + \sum_{k=2,4} F^k(\mathrm{fd}) f_k(\mathrm{fd}) + \sum_{k=1,3,5} G^k(\mathrm{fd}) g_k(\mathrm{fd}) + \zeta_d A_{\mathrm{so}}(\mathrm{d}) \\ &+ \sum_{k=2,4,} B^k_q(\mathrm{d}) C^{(k)}_q(\mathrm{d}). \end{aligned} \tag{5}$$

Transitions between the $4f^n$ and $4f^{n-1}5d$ configurations are vibronically broadened, so detailed fitting is not possible, and a mixture of atomic calculations and fitting "by eye" has been used in most cases [3].

Since the $5d$ orbitals are much more extensive radially than the $4f$ they interact more strongly with the ligands, and the crystal-field parameters are generally about 40 times larger. Whereas for $4f^n$ the crystal-field is a small perturbation, for $4f^{n-1}5d$ it is comparable with the Coulomb interaction, and dominates the spectra.

2.3. Hyperfine Calculations

Hyperfine interactions between the electronic and nuclear states give small splittings which generally require high-resolution techniques to measure. Analysis is typically done with spin Hamiltonians, as in EPR analyses [5, 17]. However, tensor-operator techniques may be used to derive additions to the Hamiltonian that may be simply applied to all transitions. See, for example, [18, 19, 20, 21]. This approach has the advantage that it is not necessary to fit spin-Hamiltonian parameters for each electronic level separately. If spin-Hamiltonian parameters are required, they may be derived from the crystal-field calculation.

2.4. Magnetic fields and a solution to the low-symmetry problem

The effects of magnetic fields are an important diagnostic tool, and, along with hyperfine interactions, crucial to applications such as quantum information [22, 23].

Early optical work concentrated on the magnetic-splitting g values along particular directions. In high-symmetry crystals measurements along one or two directions, typically parallel and perpendicular to the symmetry axis, are

enough to completely determine the magnetic response. However, in low symmetries this is not the case. High-resolution laser experiments may be used to generate rotation curves for the magnetic splittings, and hence determine the g tensors describing the magnetic properties of the ground and excited states [17], analogous to EPR analyses [5].

The fitting of crystal-field parameters to systems with low site symmetries is a difficult problem. In the complete absence of symmetry there are 27 crystal-field parameters (including real and imaginary parts), and it is not possible to determine them from energy-level data alone. Not only do rotations of the axes lead to the same energy levels [24], but the energy-levels are often not sensitive to the phases of off-diagonal matrix elements. For this reason, many crystal-field analyses use a higher symmetry than the actual site symmetry. For example, for LaF_3 it is usual to restrict the parameters to be real [8], equivalent to using C_{2v}, rather than the actual C_2, symmetry.

Recent work by Horvath and co-workers [25, 26] has demonstrated a way forward. By adding magnetic splitting data to the fitting process, it is possible to determine parameters even in such low-symmetry crystals such as yttrium orthosilicate (YSO), which is an important material for quantum-information applications [22, 23]. What makes this approach tractable is that the magnetic splitting data for each electronic level contains significant geometric data. In low symmetries each g tensor has six independent components [5]. Adding this magnetic splitting data for several electronic states can give enough information to uniquely determine the crystal-field parameters.

2.5. Extending and simplifying the analysis

There are many interesting effects and analyses that we do not have space to cover here. For example, in the late 1960s it became clear that correlation effects could give rise to two-body crystal-field interactions, which give additional parameters [27, 28, 29], and additional insight into electronic structure.

In some cases simple models can be extremely powerful. In the early 2000's Dorenbos realised that it was possible to develop parametrizations for key energies, such as the lowest energy of the $4f^{n-1}5d$ configuration [30, 31]. These analyses are possible because the free-ion parameters are almost independent of the host, and the crystal-field and free-ion parameters have predictable trends across the series (with the 5d parameters varying much less than 4f). Consequently, from measurements for one ion, it is possible to predict the values for other ions.

3. Transition intensities

In 1962 Judd [13] and Ofelt [32] published detailed analyses of transition probabilities within the $4f^n$ configuration. The first applications were to total intensities of transitions between J multiplets. However, J. D. Axe [33] examined transitions between crystal-field levels soon after, and also did the first calculations for two-photon processes [34]. In the absence of an odd-parity interaction with the crystal, electric-dipole transitions within the $4f^n$ configuration

are forbidden. Early work considered only the mixing of atomic configurations by the crystal field but subsequent work, summarized in Ref. [35], indicated that excitations involving ligand states (dynamic polarization and charge transfer) were also important. Over the following decades, significant progress was made in both phenomenological modelling, and the understanding the underlying mechanisms, for both one-photon [2, 36, 37, 38] and two-photon transitions [39, 40]. Here we provide a brief overview. Further details may be found in Ref. [37, 38].

Spectroscopic experiments measure observables such as oscillator strengths, absorption cross sections, branching ratios, and radiative lifetimes. These observables may, in principle, be calculated from squares of matrix elements of electric-dipole, magnetic-dipole, and higher-order operators. A comprehensive discussion of these basic principles may be found in Ref. [41, 42, 43, 38].

The electric dipole operator is

$$-eD_q^{(1)} = -erC_q^{(1)}, \tag{6}$$

and the magnetic dipole operator

$$M_q^{(1)} = \frac{-e\hbar}{2mc}\left(L_q^{(1)} + 2S_q^{(1)}\right). \tag{7}$$

In these equations $C_q^{(1)}$ is a spherical tensor operator and r is the distance from the origin. The other operators and physical constants have their usual meanings. We consider only electric dipole and magnetic dipole transitions in what follows. Electric quadrupole contributions to the transition intensities are also possible [44] but are usually too small to be significant.

For linearly polarized light there is no interference between electric dipole and magnetic dipole moments, so the observables may be evaluated by adding the contributions fro m electric and magnetic dipole strengths. However, for circularly polarized light interference is possible, leading to circular dichroism and circularly polarized luminescence [45, 38, 46].

Derivations of the selection rules for optical transitions may be found in many references [12, 47, 42, 43, 48, 2]. For a recent discussion see [38].

The initial and final states need not be pure electronic states, but may be combinations of electronic and vibrational (vibronic) states. If the vibrational part of the wavefunction does not change during the transition then it may be ignored. However, if it does change then it is necessary to use wavefunctions that include both electronic and vibrational parts.

There are two particular cases of interest. The first case applies to transitions within the $4f^n$ configuration. In this case the coupling to the lattice is almost identical for the initial and final states. As a result, vibronic transitions are weak, and generally only become important for centrosymmetric systems, where purely electronic electric-dipole transitions are forbidden. The other case applies to transitions between the $4f^n$ configuration and the $4f^{n-1}5d$ configuration or charge-transfer states. In this case the coupling to the lattice is very different for the initial and final states and transitions may involve a change of several

quanta of vibration. For details the reader is referred to Section 2.2.3 of Ref. [38] and other references, such as [49, 50].

3.1. Allowed electric- and magnetic-dipole transitions

Magnetic-dipole (MD) transitions within the $4f^n$ configuration and electric-dipole (ED) transitions between the $4f^n$ and $4f^{n-1}5d$ configurations are allowed by parity selection rules [38], so it is relatively straightforward to calculate the intensities. As discussed above, for transitions between the $4f^n$ and $4f^{n-1}5d$ configurations there is considerable vibronic broadening. In many cases it is adequate to represent this by a Gaussian function, though more sophisticated approaches are also possible [49, 50].

3.2. One photon transitions within the $4f^n$ configuration

As in the case of energy-level calculations, most analyses of ED transitions within the $4f^n$ configuration rely on parametrization schemes, making use of effective operators and perturbation theory. Here we will concentrate on some key issues. The reader is referred to Refs. [37, 38], and references therein, for further details.

The electric-dipole moment vanishes between pure $4f^n$ states, so instead of the dipole moment operator $D_q^{(1)}$ an *effective* dipole moment operator is required. This may be derived from a perturbation expansion for a general effective operator:

$$D_{\mathrm{eff},q} = D_q^{(1)} + D_q^{(1)} \sum_{\beta \notin \mathrm{M}} \frac{|\beta\rangle\langle\beta|V}{E_0 - E_\beta^{(0)}} + \sum_{\beta \notin \mathrm{M}} \frac{V|\beta\rangle\langle\beta|}{E_0 - E_\beta^{(0)}} D_q^{(1)} + \ldots \qquad (8)$$

In this equation the $|\beta\rangle$ are excited states on the rare-earth *or* ligand. This operator is evaluated within the $4f^n$ model space (M). In this case, the first-order term, $D_q^{(1)}$, vanishes because this odd-parity operator cannot connect states of the same parity.

As discussed in Appendix A of Ref. [7], and Ref. [51], the denominators in the two summations in equation (8) are equal term by term and the effective operator is Hermitian. Time-reversal and Hermiticity symmetry restricts the one-electron phenomenological crystal field to even-rank operators (see, for example, Chapter 1 of [7] and Ref. [52]). The same argument may be applied to the effective dipole-moment operator, so only even-rank operators are required to parametrize the one-electron, spin-independent, part of the effective dipole-moment operator. Since they are one-electron operators for the $4f^n$ configuration, with $l = 3$ the rank of the effective operators is restricted to be less than or equal to 6.

3.3. Transitions between crystal-field levels

Judd [13] and Ofelt [32] derived parametrizations based on the perturbation-theory expansion (8). An adaption of their parametrization by Reid and Richardson [53, 54] is now in common use. The effective electric dipole moment operator

is written as

$$D_{\mathrm{eff},q} = \sum_{\lambda,t,p} A^{\lambda}_{tp} U^{(\lambda)}_{p+q} (-1)^q \langle \lambda(p+q), 1 -q | tp \rangle, \tag{9}$$

with $\lambda = 2,\ 4,\ 6,\ t = \lambda - 1,\ \lambda,\ \lambda + 1$ and p restricted by the site symmetry. In this expression, t and p are the angular-momentum labels for the odd-parity potential felt by the rare-earth ion, q is the polarization of the light, and λ and $p + q$ are the angular-momentum labels for the operator that acts on the 4f electrons. Under the superposition approximation (Section 4), which is implicit in the point-charge potentials considered by Judd and Ofelt, parameters with $t = \lambda$ are zero.

Equation (8) indicates that the effective dipole moment arises from coupling the dipole moment operator $D^{(1)}_q$ with the perturbation operator V. Since the perturbation is a scalar of the site symmetry, the A^{λ}_{tp} are non-zero only if $|tp\rangle$ (or linear combinations of $|tp\rangle$) transforms as the identity irreducible representation of the site symmetry group. Equation (9) emphasizes the coupling between the perturbation (transforming as $|tp\rangle$), and the dipole moment operator (transforming as $1q$) to give an effective operator (transforming as $|\lambda(p+q)\rangle$).

3.4. Transitions between J multiplets

The vast majority of transition-intensity analyses are for measurements of total J-multiplet to J-multiplet transitions, at room temperature, and often in solutions. Judd [13] showed that in these cases the intensities may be fitted to a three-parameter linear model, which is straight-forward to apply. The standard parameters are now labeled Ω_λ, with $\lambda = 2,\ 4,\ 6$ [35, 2]. Consider transitions from an initial multiplet $|\alpha_I J_I\rangle$ to a final multiplet $|\alpha_F J_F\rangle$. If all components of the initial multiplet are assumed to be equally populated (a good approximation at room temperature) then it is possible to average over all polarizations, sum the dipole strength over the M components of the multiplets, and use the orthogonality of $3j$ symbols to derive an expression for the dipole strength proportional to

$$\sum_{\lambda} \Omega_\lambda \langle \alpha_F J_F \| \mathbf{U}^{(\lambda)} \| \alpha_I J_I \rangle^2, \tag{10}$$

with

$$\Omega_\lambda = \sum_{t,p} \frac{1}{2\lambda + 1} \left| A^{\lambda}_{tp} \right|^2. \tag{11}$$

Note that the reduced matrix elements in equation (10) are "intermediate-coupled", i.e. the eigenvectors of the free-ion Hamiltonian have been calculated and the matrix elements are taken between these eigenvectors.

The parametrization (10) has the virtue of being linear in the Ω_λ parameters which makes fitting to experimental data straightforward, and thousands of papers have used this parametrization. In forming the sum and reducing the parametrization to just three parameters a considerable amount of information is

lost, since each Ω_λ parameter is a combination of A^λ_{tp} parameters with $t = \lambda-1$, λ, $\lambda+1$ and vibronic intensity is absorbed into the Ω_λ parametrization. Thus these parameters are not ideal for tests of models, or ab-initio calculations. Also, the assumption that the states of the initial multiplet are evenly populated may not be accurate in some cases. Nevertheless, the relative simplicity of the measurements and calculations have permitted extremely useful analyses of huge amounts of experimental data.

The multiplet-multiplet parametrization can give important input to materials engineering. Many applications require particular transitions to be strong or weak, and Judd's parametrization can often be used to evaluate the feasibility of such manipulations. For example, from Table 1 of Ref. [55] we can conclude that in Pr^{3+} transitions from the $^1G_4$ multiplet to the $^3H_4$ multiplet will always be weaker than transitions to $^3H_5$ and $^3H_6$ in *any* material.

3.5. Other processes

The theory discussed above may be extended to other processes, such as two-photon absorption and Raman scattering [56, 39, 57]. Non-radiative excitation and energy transfer processes may also be modeled [7].

4. The superposition model

The superposition model, developed by Newman and co-workers in the late 60s [52, 58, 59], is an important framework for understanding both crystal-field and intensity parameters. The idea is to use the approximation that the contributions to the effective potential from different ligands is superposable (obviously for an electrostatic potential this is exact). If we had only one ligand on the Z axis at distance R_0 only crystal-field parameters with $q = 0$ would be non-zero, due to the cylindrical symmetry. We define the *intrinsic* parameters, $\bar{B}_k(R_0)$ as those $B^{(k)}_0$ parameters for this single ligand. Adding together the effects of all the ligands yields

$$B^k_q = \sum_L \bar{B}_k(R_0)(-1)^q C^{(k)}_{-q}(\theta_L, \phi_L) \left(\frac{R_0}{R_L}\right)^{t_k}. \tag{12}$$

Here $(-1)^q C^{(k)}_{-q}(\theta_L, \phi_L)$ is required to take into account the effect of rotating a ligand from the Z axis to orientation (θ_L, ϕ_L). This angular term has the same form as in a point-charge model. The term $(R_0/R_L)^{t_k}$, which takes into account the variation of the interactions with distance, would be the same as for a point-charge potential if we chose $t_k = k + 1$. However, analyses of experimental crystal-field parameters suggest that the power law is generally higher than electrostatic power laws. This is because the quantum-mechanical effects that give rise to the majority of the "crystal field" involves overlap of ligand orbitals, which fall off faster than electrostatic potentials. An important feature of the superposition model is that by reducing the parametrization to single ligands it is possible to compare crystal-field interactions between sites of different

symmetry. For detailed discussion of such applications see the papers and book by Newman and co-workers [52, 58, 59].

The superposition model may also be applied to intensity parameters [60, 61]. Under the superposition approximation the A^{λ}_{tp} intensity parameters with $t = \lambda$ are zero. In crystals with simple ionic ligands these parameters appear to be small but in some systems, particularly those with polarizable bonds close to the rare-earth ion, the superposition model breaks down [62], and parameters with $t = \lambda$ are required to fit the data. The relative signs of fitted intensity parameters give important information. We have suggested that these signs give restrictions on the possible mechanisms contributing to the transition intensities [63]. For further details the reader is referred to Refs. [37, 38].

5. Ab-initio calculations

Atomic ab-initio calculations can now give a very accurate description of the free-ion energy levels and parameters [64, 65]. However, the vast majority of energy-level and transition-intensity calculations for $4f^n$ configurations of rare-earth ions in solids or solutions make use of the parametrized "crystal-field" Hamiltonian, and it is common to invoke a point-charge model when attempting to rationalize the crystal-field parameters. However, even in the early 60s [66] it was clear that quantum-mechanical effects were important.

Newman and co-workers performed a number of calculations of increasing sophistication in the 60s, 70s, and 80s [67, 68, 69]. Those calculations used specialized computer code. However, advances in quantum-chemistry packages have made good-quality calculations practical with standard codes. An extensive set of calculations by Ogasawara and co-workers is described in Ref. [70]. Recent calculations by Seijo, Barandiarán, and coworkers (see Chapter 285 of this volume) give excellent agreement with experiment. See, for example, their calculations for $SrCl_2$:Yb^{2+} in Ref. [71, 72].

These ab-initio calculations give energy levels, not parameters. This limits their usefulness. Energy levels are restricted to a single ion, whereas parameters can be interpolated and extrapolated to other ions, and used for further calculations or analysis. Though it is possible to fit the effective Hamiltonian parameters to calculated energy levels, as in [65, 73], it is desirable to have a more robust method.

We have shown that that it is possible to construct an effective Hamiltonian matrix from *ab initio* calculations [74, 75, 76], and hence determine crystal-field and other parameters by a straightforward projection technique. The crystal-field parameters obtained by this method with modern quantum-chemical codes are quite accurate. We give an example of a calculation for Ce^{3+} in $LiYF_4$ in Table 1. Recently this method has been used to calculate parameters for a variety of Ce^{3+} systems [77], notably YSO [78], where excellent agreement with EPR data is obtained despite the complete lack of site symmetry.

Ce^{3+} systems have only one valence electron. It is possible to use known trends across the rare-earth series to estimate parameters for other ions, but

Table 1: Crystal-field parameters for the $4f^1$ and $5d^1$ configurations of Ce^{3+} in $LiYF_4$. Units are cm^{-1}. From Ref. [77]. Note that the experimental fit approximated the actual symmetry by choosing all parameters to be real.

Parameter	Experiment	Theory
$B_0^2(4f)$	481	310
$B_0^4(4f)$	−1150	−1104
$B_4^4(4f)$	−1228	−1418
$B_0^6(4f)$	−89	−70
$B_4^6(4f)$	−1213	$-1140 + 237i$
$B_0^2(5d)$	4673	4312
$B_0^4(5d)$	−18649	−18862
$B_4^4(5d)$	−23871	−23871

detailed comparisons for complex systems may give important insights. For systems with more than one valence electron it is not straightforward to apply the projection method to transform from the eigenstates of the ab-initio calculations to a crystal-field basis. We anticipate that these technical problems will be solved in the near future. In the meantime, parameters may be obtained by fitting the ab-initio energies to a crystal-field model [73].

6. Conclusions

The crystal-field and transition-intensity models described in this Chapter were the result of decades of development, drawing on a variety of theoretical techniques, including group theory, atomic structure theory, and quantum chemistry. Extensive experimental data was required to determine the parameters in the models. Advances in technology have been important to this effort, with conventional spectroscopy and EPR spectroscopy supplemented by laser and synchrotron spectroscopy.

Crystal-field and transition-intensity models have been crucial to the understanding and application of optical properties of rare-earth ions. The applications are numerous and we have only been able to hint at the usefulness of the models in optical engineering.

There are two recent developments that we would like to emphasize. One is the use of magnetic-splitting data to supplement optical data as input to crystal-field fits. Low-symmetry systems such as YSO, doped with rare-earths, have potential as components of quantum-information devices, and good crystal-field modeling will aid the analysis required for optimization. The other development is the advances in ab-initio techniques. Accurate ab-initio calculations are now possible, though far from routine, and it is possible to use these calculations to predict positions and intensities of transitions. This has obvious potential for design of materials for phosphor and other applications.

For many decades, the richness of rare-earth spectra have offered the tantalizing possibility of deriving local structure from spectra. Current developments

in modeling and ab-initio calculations are close making this dream a reality.

Acknowledgments

It has been a pleasure to have known some of the people who made crucial contributions to this field in the 1950s and 1960s, several of whom are no longer with us. I would like to particularly acknowledge the generous help and encouragement that that I received early in my career from Brian Wybourne, Brian Judd, Bill Carnall, Hannah Crosswhite, and Doug Newman. I would also like to thank my numerous co-workers who have made working in this area so enjoyable.

References

[1] C. Görller-Walrand, K. Binnemans, Rationalization of crystal–field parameterization, in: J. K. A. Gschneidner, L. Eyring (Eds.), Handbook on the Physics and Chemistry of Rare Earths, Vol. 23, North-Holland, Amsterdam, 1996, Ch. 155, pp. 121–283.

[2] C. Görller-Walrand, K. Binnemans, Spectral intensities of $f-f$ transitions, in: K. A. Gschneidner, Jr., L. Eyring (Eds.), Handbook on the Physics and Chemistry of the Rare Earths, Vol. 25, North Holland, Amsterdam, 1998, Ch. 167, pp. 101–264.

[3] G. W. Burdick, M. F. Reid, $4f^N \rightarrow 4f^{N-1}5d$ transitions, in: K. A. Gschneidner Jr., J. C. Bünzli, V. K. Percharsky (Eds.), Handbook on the Physics and Chemistry of the Rare Earths, Vol. 37, North Holland, 2007, Ch. 232, pp. 61–91.

[4] H. Bethe, Termaufspaltung in kristallen, Annalen der Physik 395 (1929) 133–208.

[5] A. Abragam, B. Bleaney, Electron paramagnetic resonance of transition ions, Clarendon Press, Oxford, 1970.

[6] G. H. Dieke, Spectra and energy levels of rare earth ions in crystals, Interscience, 1968.

[7] G. Liu, B. Jacquier (Eds.), Spectroscopic Properties of Rare Earths in Optical Materials, Springer, 2005.

[8] W. Carnall, G. Goodman, K. Rajnak, R. Rana, A systematic analysis of the spectra of the lanthanides doped into single crystal LaF_3, J. Chem. Phys. 90 (1989) 3443–3457.

[9] K. Rajnak, Configuration-interaction effects on the "free-ion" energy levels of Nd^{3+} and Er^{3+}, J. Chem. Phys. 847-855.

[10] B. R. Judd, Three-particle operators for equivalent electrons, Phys. Rev. 141 (1966) 4–14.

[11] B. Ng, D. J. Newman, Many-body crystal field calculations I: Methods of computation and perturbation expansion, J. Chem. Phys. 87 (1987) 7110–7117.

[12] B. G. Wybourne, Spectroscopic properties of rare earths, Wiley-Interscience, New York, 1965.

[13] B. R. Judd, Optical absorption intensities of rare–earth ions, Phys. Rev. 127 (1962) 750–761.

[14] T. S. Piper, J. P. Brown, D. S. McClure, fd and $f^{13}d$ configurations in a crystal field and the spectrum of Yb^{++} in cubic crystals, J. Chem. Phys. 46 (1967) 1353–1358.

[15] L. van Pieterson, M. F. Reid, R. T. Wegh, S. Soverna, A. Meijerink, $4f^n \rightarrow 4f^{n-1}5d$ transitions of the light lanthanides: experiment and theory, Phys. Rev. B 65 (2002) 045113.

[16] L. van Pieterson, M. F. Reid, G. W. Burdick, A. Meijerink, $4f^n \rightarrow 4f^{n-1}5d$ transitions of the heavy lanthanides: experiment and theory, Phys. Rev. B 65 (2002) 045114.

[17] Y. Sun, T. Böttger, C. W. Thiel, R. L. Cone, Magnetic g tensors for the $^4I_{15/2}$ and $^4I_{13/2}$ states of Er^{3+}:Y_2SiO_5, Phys. Rev. B 77 (2008) 085124.

[18] D. P. McLeod, M. F. Reid, Intensities of hyperfine transitions of Pr^{3+} and Ho^{3+} in CaF_2, J. Alloys Comp. 250 (1997) 302–305.

[19] J.-P. R. Wells, G. D. Jones, M. F. Reid, M. N. Popova, E. P. Chukalina, Hyperfine patterns of infrared absorption lines of Ho^{3+} C_{4v} centres in CaF_2, Mol. Phys. 102 (2004) 1367–1376.

[20] O. Guillot-Noel, Y. Le Du, F. Beaudoux, E. Antic-Fidancev, M. F. Reid, R. Marino, J. Lejay, A. Ferrier, P. Goldner, Calculation and analysis of hyperfine and quadrupole interactions in praseodymium-doped $La_2(WO_4)_3$, J. Luminescence 130 (2010) 1557–1565.

[21] D. S. Pytalev, E. P. Chukalina, M. N. Popova, G. S. Shakurov, B. Z. Malkin, S. L. Korableva, Hyperfine interactions of Ho^{3+}:KY_3F_{10}: Electron paramagnetic resonance and optical spectroscopy studies, Phys. Rev. B 86 (2012) 115124.

[22] P. Goldner, A. Ferrier, O. Guillot-Nöel, Rare earth-doped crystals for quantum information processing, in: J. C. Bunzli, V. K. Percharsky (Eds.), Handbook on the Physics and Chemistry of the Rare Earths, Vol. 46, North Holland, 2015, Ch. 267, pp. 1–78.

[23] M. Zhong, M. P. Hedges, R. L. Ahlefeldt, J. G. Bartholomew, S. E. Bevan, S. M. Wittig, J. J. Longdell, M. J. Sellars, Optically addressable nuclear spins in a solid with a six-hour coherence time, Nature 517 (2015) 177–181.

[24] G. W. Burdick, M. F. Reid, Crystal field parametrizations for low symmetry systems, Mol. Phys. 102 (2004) 1141–1147.

[25] S. P. Horvath, M. F. Reid, J. P. R. Wells, M. Yamaga, High precision wavefunctions for hyperfine states of low symmetry materials suitable for quantum information processing, J. Luminescence 169 (2016) 773–776.

[26] S. P. Horvath, High-resolution spectroscopy and novel crystal-field methods for rare-earth based quantum information processing, Ph.D. thesis, University of Canterbury, Christchurch, New Zealand (2016).

[27] D. J. Newman, S. S. Bishton, Theory of the correlation crystal field, Chem. Phys. Lett. 1 (1968) 616–618.

[28] B. R. Judd, Correlation crystal fields for lanthanide ions, Phys. Rev. Lett. 39 (1977) 242–244.

[29] M. F. Reid, D. J. Newman, Correlation crystal fields, in: D. J. Newman, B. Ng (Eds.), Crystal Field Handbook, Cambridge University Press, 2000, Ch. 6, pp. 122–141.

[30] P. Dorenbos, The 5d level positions of the trivalent lanthanides in inorganic compounds, J. Luminescence 91 (2000) 155–176.

[31] P. Dorenbos, Relation between Eu^{2+} and Ce^{3+} f $\leftrightarrow$ d-transition energies in inorganic compounds, J. Phys. Condens. Matter 15 (2003) 4797–4807.

[32] G. S. Ofelt, Intensities of crystal spectra of rare–earth ions, J. Chem. Phys. 37 (1962) 511–520.

[33] J. D. Axe, Radiative transition probabilities within $4f^n$ configurations: the fluorescence spectrum of europium ethylsulphate, J. Chem. Phys. 39 (1963) 1154–1160.

[34] J. D. Axe, Two–photon processes in complex atoms, Phys. Rev. 136A (1964) 42–45.

[35] R. D. Peacock, The intensities of lanthanide f—f transitions, Struct. Bonding 22 (1975) 83–122.

[36] L. Smentek, Theoretical description of the spectroscopic properties of rare earth ions in crystals, Phys. Rep. 297 (1998) 155–237.

[37] M. F. Reid, Transition intensities, in: D. J. Newman, B. Ng (Eds.), Crystal Field Handbook, Cambridge University Press, 2000, Ch. 10, pp. 193–230.

[38] M. F. Reid, Transition intensities, in: G. Liu, B. Jacquier (Eds.), Spectroscopic Properties of Rare Earths in Optical Materials, Springer, 2005, Ch. 2, pp. 95–127.

[39] M. C. Downer, The puzzle of two-photon rare earth spectra in solids, in: W. M. Yen (Ed.), Laser Spectroscopy of Solids II, Springer-Verlag, Berlin, 1989, pp. 29–75.

[40] A. D. Nguyen, Polarization dependence of two-photon absorption and electronic raman scattering intensities in crystals, Phys. Rev. B 55 (1997) 5786–5798.

[41] M. Weissbluth, Atoms and Molecules, Academic Press, New York, 1978.

[42] S. B. Piepho, P. N. Schatz, Group theory in spectroscopy, with applications to magnetic circular dichroism, Wiley, New York, 1983.

[43] B. Henderson, G. F. Imbusch, Optical spectroscopy of inorganic solids, Clarendon Press, Oxford, 1989.

[44] P. A. Tanner, G. G. Siu, Electric quadrupole allowed transitions of lanthanide ions in octahedral symmetry, Mol. Phys. 75 (1992) 233–242.

[45] P. S. May, M. F. Reid, F. S. Richardson, Circular dichroism and electronic rotatory strengths of the samarium $4f$–$4f$ transitions in $Na_3[Sm(oxydiacetate)_3] \cdot 2NaClO_4 \cdot 6H_2O$, Mol. Phys. 62 (1987) 341–364.

[46] J. P. Riehl, G. Muller, Circularly polarized luminescence spectroscopy for lanthanide systems, in: K. A. Gschneidner, Jr., J. C. Bunzli, V. K. Percharsky (Eds.), Handbook on the Physics and Chemistry of the Rare Earths, Vol. 34, North Holland, 2004, Ch. 220, pp. 289–357.

[47] S. Hüfner, Optical spectra of transparent rare earth compounds, Academic Press, 1978.

[48] G. E. Stedman, Diagram techniques in group theory, Cambridge University Press, Cambridge, 1990.

[49] G. K. Liu, X. Y. Chen, N. M. Edelstein, M. F. Reid, J. Huang, Analysis of f-element multiphonon vibronic spectra, J. Alloys Comp. 366 (2004) 240–244.

[50] M. Karbowiak, A. Urbanowicz, M. F. Reid, $4f^6 \rightarrow 4f^5 5d^1$ absorption spectrum analysis of Sm^{2+}: $SrCl_2$, Phys. Rev. B 76 (2007) 115125.

[51] A. R. Bryson, M. F. Reid, Transition amplitude calculations for one- and two-photon absorption, J. Alloys Comp. 275-277 (1998) 284–287.

[52] D. J. Newman, Theory of lanthanide crystal fields, Adv. Phys. 20 (1971) 197–256.

[53] M. F. Reid, F. S. Richardson, Anisotropic ligand polarizability contributions to lanthanide $4f$–$4f$ intensity parameters, Chem. Phys. Lett. 95 (1983) 501–507.

[54] M. F. Reid, F. S. Richardson, Lanthanide $4f$–$4f$ electric dipole intensity theory, J. Phys. Chem. 88 (1984) 3579–3586.

[55] L. Aarts, B. van der Ende, M. F. Reid, A. Meijerink, Downconversion for solar cells in YF_3:Pr^{3+}, Yb^{3+}, Spectroscopy Letters 43 (2010) 373–381.

[56] B. R. Judd, D. R. Pooler, Two-photon transitions in gadolinium ions, J. Phys. C 15 (1982) 591–598.

[57] P. C. Becker, N. Edelstein, G. M. Williams, J. J. Bucher, R. E. Russo, J. A. Koningstein, L. A. Boatner, M. M. Abraham, Intensities and asymmetries of electronic Raman scattering in $ErPO_4$ and $TmPO_4$, Phys. Rev. B 31 (1985) 8102–8110.

[58] D. J. Newman, B. Ng, The superposition model of crystal fields, Rep. Prog. Phys. 52 (1989) 699–763.

[59] D. J. Newman, B. K. C. Ng (Eds.), Crystal Field Handbook, Cambridge University Press, Cambridge, 2000.

[60] D. J. Newman, G. Balasubramanian, Parametrization of rare–earth ion transition intensities, J. Phys. C: Solid State Phys. 8 (1975) 37–44.

[61] M. F. Reid, F. S. Richardson, Electric dipole intensity parameters for lanthanide $4f$–$4f$ transitions, J. Chem. Phys. 79 (1983) 5735–5742.

[62] M. F. Reid, F. S. Richardson, Anisotropic ligand polarizability contributions to lanthanide $4f$–$4f$ intensity parameters, Chem. Phys. Lett. 95 (1983) 501–507.

[63] M. F. Reid, J. J. Dallara, F. S. Richardson, Comparison of calculated and experimental $4f$–$4f$ intensity parameters for lanthanide complexes with isotropic ligands, J. Chem. Phys. 79 (1983) 5743–5751.

[64] J. C. Morrison, K. Rajnak, Many-body calculations for heavy atoms, Phys. Rev. A 4 (1971) 536–542.

[65] C. K. Duan, M. F. Reid, S. Xia, Parameterized analysis of the ab initio calculation of Pr^{3+} energy levels, J. Luminescence 122 (2007) 939–941.

[66] C. K. Jørgensen, R. Pappalardo, H.-H. Schmidtke, Do the "ligand field" parameters in lanthanides represent weak covalent bonding?, J. Chem. Phys. 39 (1963) 1422–1430.

[67] M. Ellis, D. J. Newman, Crystal field in rare-earth trichlorides I. Overlap and exchange effects in $PrCl_3$, J. Chem. Phys. 47 (6) (1967) 1986–1993.

[68] B. Ng, D. J. Newman, *Ab–initio* calculation of crystal field correlation effects in Pr^{3+}–Cl^-, J. Phys. C: Solid State Phys. 19 (1986) L585–588.

[69] M. F. Reid, B. Ng, Complete second-order calculations of intensity parameters for one-photon and two-photon transitions of rare-earth ions in solids, Mol. Phys. 67 (1989) 407–415.

[70] K. Ogasawara, S. Watanabe, H. Toyoshima, M. G. Brik, First-principles calculations of $4f^n \rightarrow 4fn15d$ transition spectra, in: K. A. Gschneidner Jr., J. C. Bunzli, V. K. Percharsky (Eds.), Handbook on the Physics and Chemistry of the Rare Earths, Vol. 37, North Holland, 2007, Ch. 231, pp. 1–59.

[71] G. Sánchez-Sanz, L. Seijo, Z. Barandiarán, Yb^{2+}-doped $SrCl_2$: Electronic structure of impurity states and impurity-trapped excitons, J. Chem. Phys. 133 (2010) 114509.

[72] G. Sánchez-Sanz, L. Seijo, Z. Barandiarán, Electronic spectra of Yb^{2+}-doped $SrCl_2$, J. Chem. Phys. 133 (2010) 114506.

[73] A. J. Salkeld, M. F. Reid, J. P. R. Wells, G. Sanchez-Sanz, L. Seijo, Z. Barandiaran, Effective hamiltonian parameters for ab initio energy-level calculations of $SrCl_2$:Yb^{2+} and $CsCaBr_3$:Yb^{2+}, J. Phys. Condensed Matter 25 (2013) 415504.

[74] M. F. Reid, C. K. Duan, H. Zhou, Crystal-field parameters from ab initio calculations, J. Alloys Comp. 488 (2009) 591 – 594.

[75] M. F. Reid, L. Hu, S. Frank, C. K. Duan, S. Xia, M. Yin, Spectroscopy of high-energy states of lanthanide ions, Eur. J. Inorg. Chem. (2010) 2649–2654.

[76] L. Hu, M. F. Reid, C. K. Duan, S. Xia, M. Yin, Extraction of crystal-field parameters for lanthanide ions from quantum-chemical calculations, J. Phys.-Condes. Matter 23 (2011) 045501.

[77] J. Wen, L. Ning, C.-K. Duan, Y. Chen, Y. Zhang, M. Yin, A Theoretical Study on the Structural and Energy Spectral Properties of Ce^{3+} Ions Doped in Various Fluoride Compounds, J. Phys. Chem. C 116 (2012) 20513–20521.

[78] J. Wen, C.-K. Duan, L. Ning, Y. Huang, S. Zhan, J. Zhang, M. Yin, Spectroscopic Distinctions between Two Types of Ce^{3+} Ions in X2-Y_2SiO_5: A Theoretical Investigation, J. Phys. Chem. A 118 (2014) 4988–4994.